ISSN 1990-4789, Journal of Applied and Industrial Mathematics, 2009, Vol. 3, No. 2, pp. 173–182. © Pleiades Publishing, Ltd., 2009.
Original Russian Text © Yu.A. Dashevskii, D.O. Tailakov, 2007, published in Sibirskii Zhurnal Industrial'noi Matematiki, 2007, Vol. X, No. 4, pp. 21–31.

Nondestructive Diagnostics of Living Trees Using Low Frequency Electric Tomography

Yu. A. Dashevskii* **and D. O. Tailakov**

Institute of Geophysics, pr. Akad. Koptyuga 5, Novosibirsk, 630090 Russia

Received December 7, 2006

Abstract—We develop and test on real objects a scientifically justified method for monitoring electric conductivity in living trees which is based on solving the inverse problem of dendrotomography. For the purpose of nondestructive diagnostics of the wood condition, we propose to determine the electric anisotropy coefficient of a living tree. We theoretically develop and experimentally confirm a technique for determining this parameter. We prove that the electric anisotropy coefficient is independent of the seasonal variations of resistivity and is determined by the system of annual rings of the tree.

DOI: 10.1134/S1990478909020045

INTRODUCTION

Low frequency electric tomography is widely used in various branches of science and technology. This technique is based on noninvasive electric measurements on the surface of the object under study followed by solving the inverse problem. In result, it is possible to determine and visualize the spatial distribution of specific electric resistivity inside the object [1, 2].

Some unusual applications of electric tomography are known that aim at studying the electric properties of objects in nature such as a living tree. In this case, the low frequency electric tomography is called *dendrotomography*.

The possibilities of dendrotomography were tested on the beech trees designated for felling. Our results confirm the applicability of this technique to studying the decay of trees induced by various fungal infections, as well as humidity and other factors detrimental to forests [3].

Our analysis of the dendrotomography literature allows us to make the following conclusions:

- experiments on living trees aim at detecting and localizing defective parts of the trunk,
- there is no data on the long-term monitoring of the condition of live and sound trees,
- the constructions of interpretation models fail to account for the fact that trees have a thin layer structure in the radial direction (the annual rings).

Taking all these into account, we formulated the following goals of the present study:

- to inspect the possibilities of dendrotomography basing on isotropic and anisotropic models for the distribution of specific electric resistivity inside the trunk,
- using the method of dendrotomography, conduct the year-round monitoring of the condition of a living tree.

*E-mail: yuliy.dashevsky@bakerhughes.com

1. THE POTENTIAL OF A POINT SOURCE OF DIRECT CURRENT ON THE SURFACE OF A CYLINDRICALLY LAYERED MEDIUM

In the construction of a mathematical model of dendrotomography, we should account for the inner structure of the trunk. The inner isotropic region is the *heartwood*. The outer region called *sapwood* consists of the system of annual rings and is anisotropic as regards the electric properties. As a rule, the heartwood holds the main store of water and minerals of a tree.

Consider a mathematical model of low frequency electric tomography. Start with the simplest case: a model with one dividing boundary. Take an infinite cylinder of radius a and suppose that an arbitrary source of direct current is located outside the cylinder. The source is characterized by the distribution of the external electric current density $\vec{j}_c$. Denote the resistivity of the cylinder and the outer medium by ρ_i and ρ_e respectively.

Introduce the cylindrical coordinate system $\{r, \varphi, z\}$ whose z-axis coincides with the axis of the cylinder. Represent the potential u_e of the electric field outside the cylinder in the form

$$u_e = u_0 + \tilde{u}_e.$$

Here u_0 is the potential of the electric field $\vec{j}_c$ of external currents in a homogeneous medium with resistivity ρ_e. Denote the potential inside the cylinder by u_i.

Assuming that the function u_0 is known, formulate some boundary value problem for determining the potentials $\tilde{u}_e$ and u_i. It is known that the required functions satisfy the Laplace equation. In the case of a conducting medium the potential and the normal (radial) component of the electric current density are continuous on the boundary between the cylinder and the ambient medium. In the vicinity of the source, the potential u_e tends to its value u_0 in the homogeneous medium with resistivity ρ_e, and at infinity u_e it vanishes [5].

Therefore, basing on the uniqueness theorem for the boundary value problems for the Laplace equation in an inhomogeneous medium, we arrive at the following formulation of the boundary value problem [6]:

(1) the functions $\tilde{u}_e$ and u_i satisfy the Laplace equation

$$\Delta u = 0, \quad u = \begin{cases} u_i, & r < a, \\ \tilde{u}_e, & r > a; \end{cases} \tag{1}$$

(2) on the boundary $(r = a)$ of the cylinder, we have the boundary conditions

$$u_i = u_0 + \tilde{u}_e, \tag{2}$$

$$\gamma_i \left(\frac{\partial u_i}{\partial r} \right) = \gamma_e \left(\frac{\partial u_0}{\partial r} + \frac{\partial \tilde{u}_e}{\partial r} \right), \tag{3}$$

where $\gamma_i = 1/\rho_i$ and $\gamma_e = 1/\rho_e$;

(3) in the vicinity of the source (as $R \to 0$), we have $u_e \to u_0$;

(4) at the infinite distance from the source (as $R \to \infty$), we have $u_e \to 0$.

Define the Fourier image of u with respect to the coordinate z:

$$u^*(r, \varphi, \lambda) = \int_{-\infty}^{+\infty} e^{-i\lambda z} u(r, \varphi, z)\, dz \tag{4}$$

$$u(r, \varphi, z) = \frac{1}{2\pi} \int_{-\infty}^{+\infty} e^{i\lambda z} u^*(r, \varphi, \lambda)\, d\lambda. \tag{5}$$

Expand u^* and u_0^* into the Fourier series with respect to the angular coordinate:

$$u^* = \sum_{n=0}^{\infty} u_n^{*c} \cos n\varphi + u_n^{*s} \sin n\varphi = \sum_{n=0}^{\infty} u_n^{*c,s} \begin{pmatrix} \cos n\varphi \\ \sin n\varphi \end{pmatrix}, \tag{6}$$

$$u_0^* = \sum_{n=0}^{\infty} u_{0n}^{*c} \cos n\varphi + u_{0n}^{*s} \sin n\varphi = \sum_{n=0}^{\infty} u_{0n}^{*c,s} \begin{pmatrix} \cos n\varphi \\ \sin n\varphi \end{pmatrix}. \tag{7}$$

The last equalities in the chains (6) and (7) define these brief expressions for the Fourier series used henceforth. From (1)–(3) we obtain the equation

$$\frac{\partial^2 u_n^{*c,s}}{\partial r^2} + \frac{1}{r}\frac{\partial u_n^{*c,s}}{\partial r} - \left(\frac{n^2}{r^2} + \lambda^2\right) u_n^{*c,s} = 0 \tag{8}$$

and the following boundary conditions at $r = a$:

$$u_{\text{in}}^{*c,s} = u_{0n}^{*c,s} + \tilde{u}_{\text{en}}^{*c,s}, \qquad \gamma_i \left(\frac{\partial u_{\text{in}}^{*c,s}}{\partial r}\right) = \gamma_e \left(\frac{\partial u_{0n}^{*c,s}}{\partial r} + \frac{\partial \tilde{u}_{\text{en}}^{*c,s}}{\partial r}\right). \tag{9}$$

The indices in and en mean that the terms of the Fourier series are considered for $r < a$ and $r > a$ respectively.

A solution to (8) accounting for the behavior of the potential as $r \to 0$ and $r \to \infty$ is of the form

$$u_n^{*c,s} = \begin{cases} A_n^{*c,s} I_n(mr), & r < a, \\ B_n^{*c,s} K_n(mr), & r > a. \end{cases} \tag{10}$$

Here $m = |\lambda|$, while $I_n(x)$ and $K_n(x)$ are the modified Bessel functions.

Assume that the source of the external current is pointlike, driven by the direct current of amperage I and located at the point $\{r_0, \varphi_0, z_0\}$. Inserting (10) into (9) and solving the resulting system of linear equations, we obtain the expression

$$u(\dot{\varphi}, \dot{z}, a) = \frac{I}{2\pi^2 a \gamma_e} \sum_{n=0}^{\infty} \frac{2}{\varepsilon_n} \cos(n\dot{\varphi}) \int_0^{\infty} \frac{1}{x} \frac{I_n(x) K_n(x)}{S I_n'(x) K_n(x) - K_n'(x) I_n(x)} \cos(x\dot{z})\, dx \tag{11}$$

for the potential in the case that $r = r_0 = a$, where $S = \gamma_i/\gamma_e$, $\dot{\varphi} = \varphi - \varphi_0$, $\dot{z} = (z - z_0)/a$, and $x = ma$.

Consider the case that $\rho_e = \infty$, the source of the current is located on the outer surface of the cylindrical model ($r = a$), and inside the cylinder there is another boundary ($r = b$). In the region $0 < r < b$, the medium has resistivity ρ_2. Under these conditions, the potential u for $r = a$ is of the form

$$u = \frac{I}{\pi} \sum_{n=0}^{\infty} \left[\int_0^{+\infty} \left(u_{0n}^{*c,s}(a) + A_n^{c,s} I_n(ma) + B_n^{c,s} K_n(ma) \right) \cos(ma\, \dot{z})\, dm \right] \times \begin{pmatrix} \cos n\varphi \\ \sin n\varphi \end{pmatrix}. \tag{12}$$

$$B_n^{c,s} = \frac{u_{0n}^{*c,s}(b) \frac{1}{I_n(mb)} - \frac{\partial u_{0n}^{*c,s}(b)}{\partial r} \frac{1}{mSI_n'(mb)} - \frac{\partial u_{0n}^{*c,s}(a)}{\partial r} \frac{1}{mI_n'(ma)} \left(1 - \frac{1}{S}\right)}{\left(1 - \frac{1}{S}\right) \frac{K_n'(ma)}{I_n'(ma)} - \frac{K_n(mb)}{I_n(mb)} + \frac{1}{S} \frac{K_n'(mb)}{I_n'(mb)}}, \tag{13}$$

$$A_n^{c,s} = -\frac{\partial u_{0n}^{*c,s}(a)}{\partial r} \frac{1}{mI_n'(ma)} - B_n^{c,s} \frac{K_n'(ma)}{I_n'(ma)}, \tag{14}$$

where $S = \gamma_i/\gamma_2$.

2. AN ASYMPTOTIC EXPANSION OF THE POTENTIAL AT LARGE DISTANCES FROM THE SOURCE

In the two-layer model of the medium, let us construct an asymptotic representation for the potential u in the region with the large values of $\dot{z}$. To this end, expand the integrands using the approximate values [7] of the Bessel functions as $x \to 0$. Then upon integration we obtain the approximate expression

$$u(\dot{\varphi}, \dot{z}, a) \approx \frac{I}{\pi a} \frac{1}{\gamma_e + \gamma_i} \sum_{n=0}^{\infty} \frac{1}{\varepsilon_n} \cos(n\dot{\varphi}) \frac{1}{2^{2n}(n!)^2} \frac{\partial^{2n}}{\partial \dot{z}^{2n}} \left[\frac{1}{\dot{z}}\right] \tag{15}$$

for the potential in the case that $r = r_0 = a$.

Consider the ratio $f_{n+1,n}$ of the $(n+1)$th and nth terms of the series in (15) assuming that $\dot{\varphi} = 0$ and $\dot{z} > 1$. This yields

$$f_{n+1,n} = \frac{(2n+1)(2n+2)}{4\dot{z}^2(n+1)^2} < 1. \tag{16}$$

It follows from (16) that, for $n \gg 1$, the function $f_{n+1,n}$ is essentially independent of n and decreases with the growth of $\dot{z}$ as $1/\dot{z}^2$. Inspection shows that, for $\dot{z} > 1$, we can with adequate precision restrict ourselves to taking the first three terms of (15):

$$u(\dot{z}, a) \approx u_{as} = \frac{I}{2\pi a}\frac{1}{\gamma_e + \gamma_i}\left(\frac{1}{\dot{z}} + \frac{1}{2(\dot{z})^3} + \frac{3}{4(\dot{z})^5} + \cdots\right). \tag{17}$$

Comparison of the values of the asymptotic expansion (17) and the analytic solution (11) for various ratios $S = \gamma_i/\gamma_e$ is represented in Table 1 ($\dot{\varphi} = 0$). Here, for various values of S and $\dot{z}$, we give in percentages the differences δ between the exact and approximate values of the potential:

$$\delta = |(u - u_{as})/u_{as}| \cdot 100\,\%.$$

Therefore, looking at the table, we can make a conclusion on the limits of applicability of the asymptotic representation (17).

Table 1. Comparison of exact and asymptotic values of the potential

$\dot{z}$	S				
	1.01	0.1	1	10	100
1	45.9	47.4	50.1	48.8	46.5
$\sqrt{2}$	29.4	30.5	32.0	31.6	31.0
2	24.1	24.6	25.1	24.5	24.1
$2\sqrt{2}$	18.1	19.0	20.2	19.9	19.0
4	8.5	9.6	10.5	9.6	9.1
$4\sqrt{2}$	4.9	5.2	5.7	5.4	5.0
8	1.9	2.1	2.5	2.2	2.1
$8\sqrt{2}$	0.9	1.1	1.2	1.1	1.0
16	0.8	0.9	0.9	0.9	0.8
$16\sqrt{2}$	0.2	0.2	0.3	0.2	0.2
32	0.1	0.1	0.1	0.1	0.1

The data in Table 1 allows us to conclude that, for all practically interesting values of S, the approximate representation (17) keeping the first three terms of the series can be used for describing the potential with error of order 1 % provided that $\dot{z} = z/a > 10$.

Arguing similarly, we obtain the asymptotic expansion

$$u \approx \frac{I}{\pi a}\frac{1}{\gamma_2}\sum_{n=0}^{\infty}\frac{1}{\varepsilon_n}\cos n(\varphi - \varphi_0) \times \left(\frac{2a^{2n}(1+S) + b^{2n}(1-S)}{2a^{2n}(1+S) - b^{2n}(1-S)}\right)\frac{1}{2^{2n}(n!)^2}\frac{\partial^{2n}}{\partial \dot{z}^{2n}}\left[\frac{1}{\dot{z}}\right] \tag{18}$$

for the potential (12) in the three-layer model of the medium. Analyzing the results of numerous computations, we see that in this case the limits of the applicability of (18) are determined by the condition $\dot{z} > 10$ as well.

3. A POINT SOURCE OF DIRECT CURRENT LOCATED ON THE SURFACE OF A MULTI-LAYER CYLINDRICALLY LAYERED MODEL. ISOTROPIC AND ANISOTROPIC MEDIA

Consider a model of the object under study consisting of k layers. The outer layer is some medium with the zero value of electric conductivity (like air). The other $k-1$ layers are infinite cylinders, one enclosed into another, of radii $a_1, a_2, \ldots, a_{k-1}$ and conductivities $\gamma_1, \gamma_2, \ldots, \gamma_{k-1}$. The index $k-1$ refers to the cylinder of the smallest radius, while $k=1$, to the largest radius.

Consider the problem of determining the potential $\tilde{u}_1$ on the outer boundary $r=a_1$. In order to solve the Laplace equation, on each boundary we can write two boundary conditions, which gives a system of $2(k-1)$ equations with $2(k-1)$ constants. Represent this system in the matrix form: $MX=U$. Here M is the matrix of modified Bessel functions of order n depending on the product ma_i for $i=1,\ldots,k-1$ and the coefficients $S_j=\gamma_j/\gamma_{j-1}$ for $j=1,\ldots,k-1$. The matrix X consists of the column of the required constants $C_l^{c,s}$ for $l=1,\ldots,2k-2$. The matrix U is

$$U=\begin{pmatrix} -u_{0n}^{*c,s}(a_1)\dfrac{1}{K_n(ma_1)} \\ -\dfrac{\partial u_{0n}^{*c,s}(a_1)}{\partial r}\dfrac{1}{K_n'(ma_1)} \\ u_{0n}^{*c,s}(a_2)\dfrac{1}{K_n(ma_2)} \\ \dfrac{\partial u_{0n}^{*c,s}(a_2)}{\partial r}\dfrac{1}{K_n'(ma_2)} \\ 0 \\ \ldots \\ 0 \end{pmatrix}. \tag{19}$$

In order to find the potential on the boundary, we firstly determine from $MX=U$ the functions $C_2^{c,s}$ and $C_3^{c,s}$; for instance, using the Gaussian elimination. If the values of $C_2^{c,s}$ and $C_3^{c,s}$ are known then we can express the potential at $r=a_1$ as

$$u=\frac{1}{\pi}\sum_{n=0}^{\infty}\left[\int_0^{+\infty}\left(u_{0n}^{*c,s}(a_1)+C_2^{c,s}I_n(ma_1)+C_3^{c,s}K_n(ma_1)\right)\cos(ma_1\dot{z})\,dm\right]\times\begin{pmatrix}\cos n\varphi\\ \sin n\varphi\end{pmatrix}, \tag{20}$$

where $\dot{z}=(z-z_0)/a_1$.

The solution (20) admits a generalization to the case of an anisotropic model of the medium. Consider firstly the most general model with the anisotropy of electric conductivity in three coordinates r, φ, and z for each layer but the outer one. Denote the electric conductivity along these coordinates by γ_r^j, γ_φ^j, and γ_z^j respectively (for $j=1,\ldots,k-1$). In the case under consideration, the equation for the potential u in cylindrical coordinates is of the form

$$\gamma_r^j\frac{1}{r}\frac{\partial}{\partial r}\left(r\frac{\partial u}{\partial r}\right)+\gamma_\varphi^j\frac{1}{r^2}\frac{\partial^2 u}{\partial\varphi^2}+\gamma_z^j\frac{\partial^2 u}{\partial z^2}=0. \tag{21}$$

Applying to (21) the transformations (4) and (6), we obtain

$$\frac{\partial^2 u_n^{*c,s}}{\partial r^2}+\frac{1}{r}\frac{\partial u_n^{*c,s}}{\partial r}-\left(\frac{n^2}{r^2}\left(\Lambda_{r\varphi}^j\right)^2+\lambda^2\left(\Lambda_{rz}^j\right)^2\right)u_n^{*c,s}=0, \tag{22}$$

where $\left(\Lambda_{r\varphi}^j\right)^2=\gamma_\varphi^j/\gamma_r^j$ and $\left(\Lambda_{rz}^j\right)^2=\gamma_z^j/\gamma_r^j$ are the electric anisotropy coefficients.

In the case under consideration, by analogy with (19), the matrix U is of the form

$$U = \begin{pmatrix} -u_{0n}^{*c,s}(a_1) \\ -\frac{\partial u_{0n}^{*c,s}(a_1)}{\partial r}\frac{1}{m\Lambda_{rz}^1} \\ u_{0n}^{*c,s}(a_2) \\ \frac{\partial u_{0n}^{*c,s}(a_2)}{\partial r}\frac{1}{m\Lambda_{rz}^1} \\ 0 \\ \dots \\ 0 \end{pmatrix}. \tag{23}$$

In (23), u_0 is potential of the electric field $\vec{j}_c$ of external currents in the homogeneous medium with conductivity γ_{r1}. We should stress that M includes the entries related to the anisotropy of the electric properties of the medium:

$$S_j = \frac{\gamma_r^j}{\gamma_r^{j-1}}\frac{\Lambda_{rz}^j}{\Lambda_{rz}^{j-1}}, \qquad j = 1, \dots, k-1.$$

The matrix X will be the column of required functions $C_l^{c,s}$ for $l = 1, \dots, 2k-2$. As a result we obtain the required expression for the potential:

$$u = \frac{1}{\pi}\sum_{n=0}^{\infty}\left[\int_0^{+\infty}\left[u_{0n}^{*c,s}(a_1) + C_2^{c,s}I_{n\Lambda_{r\varphi}^1}(m\Lambda_{rz}^1 a_1) + C_3^{c,s}K_{n\Lambda_{r\varphi}^1}(m\Lambda_{rz}^1 a_1)\right]\cos\left(m\Lambda_{rz}^1 a_1 \dot{z}\right)dm\right]\begin{pmatrix}\cos n\varphi \\ \sin n\varphi\end{pmatrix}. \tag{24}$$

Write an expression for the potential in the case of a three-layer model of the medium, which describes the real tree structure. Assume that the outer layer ($r > a_1$) possesses the zero conductivity (like air). The inner isotropic layer ($0 < r < a_2$) has conductivity γ_i. The intermediate anisotropic layer ($a_2 \le r \le a_1$) has different electric conductivities $\gamma_\varphi = \gamma_z = \gamma_t$ and $\gamma_r = \gamma_n$ along the coordinates r and z. In the three-layer model of the medium in question, we express (24) as

$$u = \frac{1}{\pi}\sum_{n=0}^{\infty}\left[\int_0^{+\infty}\left[u_{0n}^{*c,s}(a_1) + C_2^{c,s}I_{n\Lambda}(m\Lambda a_1) + C_3^{c,s}K_{n\Lambda}(m\Lambda a_1)\right]\cos(m\Lambda a_1 \dot{z})\,dm\right]\begin{pmatrix}\cos n\varphi \\ \sin n\varphi\end{pmatrix}. \tag{25}$$

The functions $C_2^{c,s}$ and $C_3^{c,s}$ satisfy

$$C_3^{c,s} = \frac{\frac{1}{m}\frac{\partial u_0}{\partial r}(a_2) - S_t\frac{I_n'(ma_2)}{I_n(ma_2)}u_0(a_2) - \alpha\frac{1}{m\Lambda}\frac{\partial u_0}{\partial r}(a_1)\frac{1}{I_{n\Lambda}(m\Lambda a_1)}}{S_t K_{n\Lambda}(m\Lambda a_2)\frac{I_n'(ma_2)}{I_n(ma_2)} - \alpha\Lambda K_{n\Lambda}'(m\Lambda a_2) + \frac{K_{n\Lambda}'(m\Lambda a_1)}{I_{n\Lambda}'(m\Lambda a_1)}}, \tag{26}$$

$$C_2^{c,s} = -\frac{1}{m\Lambda}\frac{\partial u_0}{\partial r}(a_1)\frac{1}{I_{n\Lambda}(m\Lambda a_1)} - C_3^{c,s}\frac{K_{n\Lambda}'(m\Lambda a_1)}{I_{n\Lambda}'(m\Lambda a_1)}. \tag{27}$$

Here

$$\alpha = \Lambda I_{n\Lambda}'(m\Lambda a_2) - S_t I_{n\Lambda}(m\Lambda a_2)/I_n'(ma_2)/I_n(ma_2), \qquad S_t = \gamma_i/\gamma_t,$$

$\Lambda = \sqrt{\gamma_t/\gamma_n}$ is the electric anisotropy coefficient of the medium, u_0 is the potential of the electric field $\vec{j}_c$ of external currents in the homogeneous medium with conductivity γ_i.

Let us continue studying the expression (25) for the potential and construct an asymptotic expansion for this function for large values of $\dot{z}$. Using the above approach to constructing asymptotics, after simple rearrangements we arrive at the following approximate expression for the potential:

$$u \approx \frac{I}{\pi a_1}\frac{1}{\gamma_t}\sum_{n=0}^{\infty}\frac{1}{\varepsilon_n}\cos n(\varphi-\varphi_0) \times \left(\frac{2a_1^{2n\Lambda}(\Lambda+S_t)+a_2^{2n\Lambda}(\Lambda-S_t)}{2a_1^{2n\Lambda}(\Lambda+S_t)-a_2^{2n\Lambda}(\Lambda-S_t)}\right)\frac{1}{2^{2n}\Lambda^{2n+1}(n!)^2}\frac{\partial^{2n}}{\partial\dot{z}^{2n}}\left[\frac{1}{\dot{z}}\right]. \tag{28}$$

In deriving this relation we assume that the source of external current is a point electrode located on the outer surface of the three-layer cylinder and fed by a current of amperage I.

Our numerical analysis of the limits of applicability of (28) for the values $\Lambda = 1, 2, 3, 4, 5$ allows us to conclude that, in all practically interesting cases, the approximate expression (28) describes the exact value of the potential with error at most 1 % provided that $\dot{z} > 10$.

4. DETERMINING THE ANISOTROPY COEFFICIENT OF THE INTERMEDIATE LAYER IN A LIVING TREE

Consider the problem of determining the anisotropy coefficient of the intermediate layer in a living tree ($a_2 \le r \le a_1$) on assuming that the measurements of the potential created by a point source of direct current are taken on the surface of a tree for all values of φ and z.

We will solve the inverse problem under the following hypotheses: Assume that the geometric characteristics a_1 and a_2 of the object under study are known. Indeed, the radius a_1 is determined by direct measurements, and some estimates for the radius of the heartwood for each tree species are available in the literature. The situation is quite different regarding the electric characteristics of the wood. We have no reason to assume known the parameters γ_t and S_t of a living tree. In order to collect this data, we would have to resort to destructive diagnostic methods.

Consider an approach which enables us to eliminate the influence of γ_t on the measurements. Let $u(z, \varphi = 0)$ denote the value of the potential taken for $\varphi = 0$. We will also use the potential $u(\varphi, z = 0)$ considered for $z = 0$. Define the function θ as

$$\theta = \frac{u(z, \varphi = 0)}{u(\varphi, z = 0)}. \tag{29}$$

By the structure of (25) and (28), it is easy that θ is independent of γ_t.

As for the degree of influence of the parameter S_t on the measurements, look at (28). This parameter occurs in the numerator and denominator of the fraction in parentheses. Consider the structure of the fraction and put

$$p_1 = a_1^{2n\Lambda}(\Lambda - S_t), \qquad p_2 = a_2^{2n\Lambda}(\Lambda - S_t).$$

Then we can write the fraction p_{12} in parentheses as $p_{12} = (p_1 - p_2)/(p_1 + p_2)$. It is not difficult to verify that $|p_{12}| < 1$; thus, the function p_{12} depends weakly on the parameters Λ and S_t.

Therefore, the dependence of the potential (28) on the anisotropy coefficient has principally to do with the parameter Λ which is outside the parentheses in (28).

This result follows from using the asymptotic expression (28) for describing the behavior of the potential. Verify the validity of this analysis for the function θ in which we use the exact expression for the potential. To this end, using (25), we calculated the value of θ for a wide range of Λ and S_t of practical interest: $1 \le \Lambda \le 8$ and $0.001 \le S_t \le 1000$.

The figure shows the dependence of θ on Λ, where all values of the function corresponding to the various values of S_t in the range are inside the narrow interval marked by the vertical segments. Therefore, as a result of numerical simulation, we prove that θ is essentially independent of the value of S_t. On this result we base the technique for determining the anisotropy coefficient while solving practical inverse problems of dendrotomography.

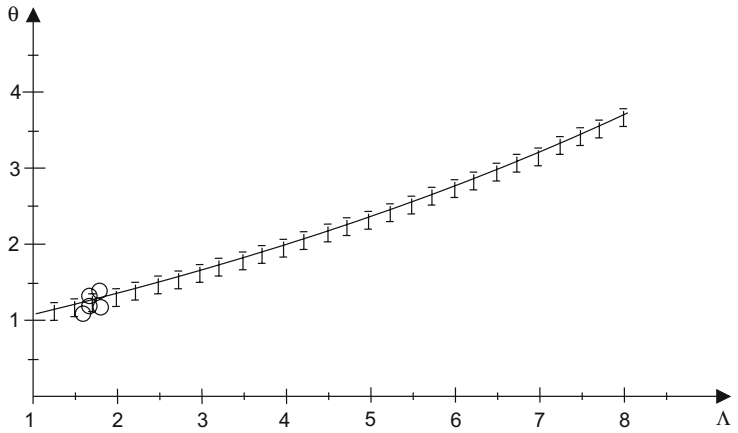

Fig. 1. The dependence of the values of θ on Λ

5. PHYSICAL EXPERIMENTS IN DENDROTOMOGRAPHY. STATEMENT AND SOLUTION OF PRACTICAL INVERSE PROBLEMS

5.1. A Laboratory Experiment

We conducted physical experiments in two stages. At the first stage for making laboratory tests we took a cylindrical vessel with diameter 0.2 m and height 0.4 m. The vessel was filled with a fluid with resistivity 18.2 Ohm·m. The resistivity of the fluid was measured at 19.4°C with a Jumo conductometer (Germany). At the distance of 0.2 m from the bottom of the vessel 16 electrodes of diameter 6 mm were uniformly spread around the perimeter, providing the galvanic contact with the fluid. The electrodes were numbered $1, \ldots, 16$.

Measurements were made using the conventional low frequency geophysical equipment Cikl-VPS and ANCh-3 produced in Russia. The mean measurement error was 4.5 %. The measurement technique was as follows: at the first step, the contacts A and B of the current generator were attached to the electrodes number $(1, 2)$. Using contacts M and N, we measured with microvoltmeters the potential difference between the pairs of electrodes $(3, 4)$, $(4, 5)$, and so on up to the pair $(15, 16)$. At the next cycle of measurements, the contacts A and B were attached to the electrodes $(2, 3)$, and the potential difference was measured sequentially between the pairs $(4, 5), (5, 6), \ldots, (16, 1)$. For 16 electrodes, the total number of measurements is equal to 208. However, by the reciprocity principle, 104 measurements suffice.

We solved the inverse problem with the laboratory data by fitting. We minimized the mean square deviation between the model and experimental data. To seek the minimum of the target functional we used the Nelder–Mead algorithm [8] that is highly reputable for solving practical inverse problems of electric probing. As the model data, we used the results of calculations using (25)–(27).

A numerical solution of the inverse problem yielded the value of the resistivity of the fluid equal to 16.7 Ohm·m. This value differs by 14 % from the test value. The difference is due to the measurement error of the signal and the deviation of the shape of the vessel from a cylinder. We should also mention another reason: neglecting the finite size of the electrodes. Accounting for this size in the models is a separate problem outside the scope of this article.

5.2. An Experiment on a Living Tree

As the object of study we chose a fir tree of diameter about 25 cm. In order to make this experiment, we implanted 23 steel electrodes with helical rifling about 6 mm deep into the crust of the tree. The mean distance between the electrodes along the circumference was 4 sm. The measurements were taken with the ANCh-3 complex. The technique of measurements remained the same as in the laboratory. We made six series of measurements, five during the period from June 2005 to November 2005, and one in May 2006. The results of the November 2005 experiment were deemed a failure as regards the precision of the measurements. This is most likely due to the suspension of the active life of the object of study, and the resulting rise in the values of the resistivity. We can assume that we actually established the time boundary between the winter "hibernation" and the spring and summer "awakening" of a living tree.

5.3. Solving the Inverse Problem

In order to solve the inverse problem and reconstruct the distribution of the resistivity, we used a numerical algorithm which realizes the solution to the direct problem of dendrotomography presented in this article. We solved the inverse problem for two classes of models of the electric properties of a living tree: isotropic and anisotropic models. The use of two classes of models is related to a fact of electric carotage theory: the equivalence of cylindrically layered anisotropic media to isotropic models [9].

Consider firstly the results of solving the inverse problem in the class of cylindrically layered isotropic models. The required unknown parameters were: the specific electric resistivity ρ_i of the heartwood; the specific electric resistivity ρ_e of the sapwood; the diameter d_2 of the heartwood. The diameter of the sapwood was assumed equal to the diameter of the trunk. As an initial approximation for the values of the resistivity parameter, we chose the resistivity of water at normal conditions. The starting value of the radius of the heartwood is equal to the half radius of the trunk. Upon solving the inverse problem the mean deviation between theoretical and experimental values was about 8 %. We established the stability of the solution with respect to the choice of the initial model.

Therefore, we reconstructed the distribution of resistivity in a living tree on assuming that the tree consists of two principal isotropic layers: heartwood and sapwood. Our results for all five series of measurements are given in Table 2.

Table 2. Solutions to the inverse problem in the class of isotropic models

Measurement dates	ρ_i, Ohm·m	ρ_e, Ohm·m	d_2, m
May 2006	26	200	0.095
June 2005	28	127	0.083
July 2005	24	52	0.045
September 2005	27	120	0.073
October 2005	25	145	0.073

Basing on these results, we can elucidate the seasonal life cycle of the tree which begins in May or June and ends in October. The peak activity of the tree is in July. The tissues exchange microelements vigorously, which results in a sharp drop (compared to June) in the resistivity and the decreasing radius of heartwood.

Consider the estimates of the anisotropy coefficient. For all five series of measurements, we numerically calculated the value of the function θ and, using the data depicted, we obtained the value of the anisotropy coefficient. The mean value of the anisotropy coefficient turned out equal to 1.7, the mean square error amounted to 9 %. The values of experimental estimates for the anisotropy coefficient for each of the five dimensions are represented in the figure as centers of the circles. The radius of a circle indicates the error in determining the corresponding parameter.

The data we present implies that there is an essential absence of the dependence of the electric anisotropy coefficient of a living tree on the season. This result has physical explanation: the radial and vertical values of the resistivity change in time synchronously; thus, the anisotropy coefficient is independent of the seasonal variations of resistivity and is determined by the structure of annual rings of the tree.

REFERENCES

1. D. C. Barber and B. H. Brown, "Applied Potential Tomography," J. Phys. Ser. E: Sci. Instrum. **17** (9), 723–733 (1984).
2. R. S. Blue, D. Isaacson, and J. C. Newell, "Real-Time Three-Dimensional Electrical Impedance Imaging," Physiol. Meas. **21**, 15–26 (2000).

3. *Dendrotomography: A Novel System for the Nondestructive Assessment of Trees*, http://www.esf.de/download/media/dendrotominfo.pdf.
4. N. E. Bulygin and V. T. Yamishko, *Dendrology* (Moscow State Forest Univ., Moscow, 2003) [in Russian].
5. Yu. A. Dashevskii, I. V. Surodina, and M. I. Epov, "Quasi-Three-Dimensional Mathematical Simulation of Diagrams of Nonaxisymmetric Direct Current Sondes in Anisotropic Media," Sibirsk. Zh. Indust. Mat. **5** (3), 76–91 (2002).
6. B. M. Budak, A. A. Samarskii, and A. N. Tikhonov, *Manual of Mathematical Physics* (Nauka, Moscow, 2002) [in Russian].
7. I. S. Gradstein and I. M. Ryzhik, *Tables of Series, Products, and Integrals*, Vols 1, 2 (Fizmatgiz, Moscow, 1963; Verlag Harri Deutsch, Frankfurt, 1981).
8. J. C. Lagarias, J. A. Reeds, M. H. Wright, and P. E. Wright, "Convergence Properties of the Nelder–Mead Simplex Method in Low Dimensions," SIAM J. Optimiz. **9** (1), 112–147 (1998).
9. K. S. Kunz and J. H. Moran, "Some Effects of Formation Anisotropy on Resistivity Measurements in Boreholes," Geophysics, **23** (4), 770–794 (1958.